



HAL
open science

Modified 3D-printed device for mercury determination in waters

Elodie Mattio, Nadia Ollivier, Fabien Robert-Peillard, Robert Di Rocco,
André Margaillan, Christophe Brach-Papa, Joel Knoery, Damien Bonne,
Jean-Luc Boudenne, Bruno Coulomb

► To cite this version:

Elodie Mattio, Nadia Ollivier, Fabien Robert-Peillard, Robert Di Rocco, André Margaillan, et al..
Modified 3D-printed device for mercury determination in waters. *Analytica Chimica Acta*, 2019,
1082, pp.78-85. 10.1016/j.aca.2019.06.062 . hal-02284950

HAL Id: hal-02284950

<https://amu.hal.science/hal-02284950>

Submitted on 12 Sep 2019

HAL is a multi-disciplinary open access archive for the deposit and dissemination of scientific research documents, whether they are published or not. The documents may come from teaching and research institutions in France or abroad, or from public or private research centers.

L'archive ouverte pluridisciplinaire **HAL**, est destinée au dépôt et à la diffusion de documents scientifiques de niveau recherche, publiés ou non, émanant des établissements d'enseignement et de recherche français ou étrangers, des laboratoires publics ou privés.

Copyright

Modified 3D-printed device for mercury determination in waters

Elodie Mattio¹, Nadia Ollivier¹, Fabien Robert-Peillard¹, Robert Di Rocco¹, Catherine Branger², André Margaillan², Christophe Brach-Papa³, Joël Knoery³, Damien Bonne⁴, Jean-Luc Boudenne¹, Bruno Coulomb^{1*}

¹ Aix Marseille Univ, CNRS, LCE, Marseille, France.

² University of Toulon, MAPIEM, La Garde, France.

³ IFREMER, LBCM, Nantes, France.

⁴ Aix Marseille Univ, CNRS, Centrale Marseille, ISM2, Marseille, France.

*Corresponding author: bruno.coulomb@univ-amu.fr

Full postal address: LCE, Case 29, 3 place Victor Hugo, 13331 Marseille cedex 3, France.

Abstract

3D printing technology is increasingly used in flow analysis, to develop low cost and tailor-made devices. The possibility of grafting specific molecules onto 3D printed parts offers new perspectives for the development of flow systems. In this study, a MPFS system including a dicarboxylate 1,5-diphenyl-3-thiocarbazone grafted 3D-printed device has been developed for mercury determination. For this purpose, the surface of 3D-printed cuboids was first modified with amine functional groups and then grafted with dicarboxylate 1,5-diphenyl-3-thiocarbazone. This new grafted device resulted in selective mercury preconcentration with extraction and elution yields higher than 90% even at high sampling flow rates. The detection can then be carried out in two ways: a direct detection of mercury extracted onto 3D-printed grafted cuboids by atomic absorption spectrophotometry after amalgam on gold or a detection of mercury in solution after elution with L-cysteine by spectrophotometry or cold vapor atomic absorption spectrometry.

Keywords: stereolithography; Poly(MethylMethacrylate) grafting; dicarboxylate 1,5-diphenyl-3-thiocarbazone; Multi Pumping Flow System; mercury.

Introduction

Mercury is one of the most toxic metal, present in the environment in different chemical forms. This post-transition metal has a high toxicity at low levels and may accumulate in organisms [1] which increases its dangerousness. The exposition to mercury can cause damages to organs [2] as respiratory and kidney diseases, dysfunctions of the nervous system [3,4] with memory troubles and developmental delay for exposed children, or troubles in the development of foetus. Mercury has the capacity to be exchanged between the different reservoirs of the biosphere [5], whether in organic or in inorganic form. There are few natural sources of mercury such as volcanism and geothermal sources [6], while anthropogenic sources are very important: mining, combustion of fossil fuels [7,8], production of batteries from mercury oxide, use in electrolytic processes for chemical or pesticides production. A recent study [9] estimated anthropic mercury in the environment at 1 540 000 tonnes, of which 73% was emitted between 1850 and 2010.

44 In the light of its toxicity and its numerous sources of pollution, the World Health Organization
45 has recommended a guideline value of $6 \mu\text{g L}^{-1}$ for inorganic mercury in drinking water and
46 European regulations have set a maximal allowable concentration (MAC) in natural waters at
47 $0.07 \mu\text{g L}^{-1}$ for mercury and its compounds. Accordingly, the development of simple, rapid and
48 sensitive methods for on-line Hg determination in natural waters has attracted widespread
49 attention in modern analytical chemistry. Flow analysis seems to be appropriate to meet these
50 specific requirements: this technology allows the decrease of instrumentation size and of
51 reagents and energy consumption, which are significant advantages to simplify the
52 manipulations required for the assays.

53 Many flow systems have been developed for quantification of mercury in waters, with a
54 detection step often performed by cold vapor atomic absorption spectrometry (CV-AAS) [10-
55 12]. Colorimetric detection has been also used for high concentrations of mercury [13,14].
56 Independently of the detection method, the quantification of low levels of mercury is usually
57 difficult because of sample storage problems [15]. A portable analytical system would avoid
58 these problems, but the coupling with complex laboratory detection techniques (atomic
59 absorption spectrometry (AAS), inductively coupled plasma mass spectrometry (ICP-MS) or
60 inductively coupled plasma atomic emission spectrometry (ICP-AES)) would remain difficult
61 to handle. A colorimetric detection step may be considered if a pre-concentration module is
62 used for low mercury concentrations.

63 3D printing eases the creation of three-dimensional custom fluidic modules as columns and
64 mixers and several flow systems based on such 3D-printed modules have been reported
65 previously for the determination of lead [16], cadmium [17] or chromium [18].

66 In this study, the 3D printing resin was used directly after the photopolymerization process as
67 a support for the grafting of a ligand for the selective extraction of mercury. Dicarboxylate 1,5-
68 diphenyl-3-thiocarbazone (DTZc) was chosen for this purpose because of its affinity for
69 mercury [19]. The grafting procedure is performed in two stages: first, amine functions are
70 integrated on the surface of the photopolymerized resin and then dicarboxylate 1,5-diphenyl-3-
71 thiocarbazone is grafted by reaction between its carboxylic function and the amine function
72 added to the resin. Various detection methods have been considered and several applications
73 are discussed here as examples to illustrate the opportunity of using a 3D printed grafted
74 module.

75

76 **2. Materials and methods**

77 **2.1. Reagents and solutions**

78 All chemicals used were of analytical grade and used without further purification. Solutions
79 were prepared with ultra-pure water (Millipore, resistivity $> 18 \text{ M}\Omega \text{ cm}$) and stocked in high
80 density polyethylene or Teflon flasks. Mercury standard solutions were prepared by dilution of
81 a commercial 1 g.L^{-1} AAS mercury stock solution (Fisher Chemical, USA) and stabilized with
82 1% v/v nitric acid trace metal grade (Fisher Chemical, USA).

83 A multi-metal solution ($10 \mu\text{mol.L}^{-1}$ for each metal) was prepared by diluting and mixing eleven
84 commercial AAS stock solutions of aluminium, cadmium, calcium, cobalt, copper, iron, lead,
85 magnesium, mercury, silver and zinc at 1 g.L^{-1} (Fisher Chemical, USA) in ultra-pure water.

86 Modification of 3D printed devices was carried out with hexane diamine (Fisher Chemical,
87 USA), N-(3-Dimethylaminopropyl)-N'-ethylcarbodiimide (EDC, GenScript, USA) and 1-
88 Hydroxybenzotriazole (HOBt, Fluka, USA).

89 Detection was performed by two techniques: spectrophotometric detection with a reagent
90 composed of dithizone (Sigma-Aldrich, USA) and thiourea (Sigma-Aldrich, USA) prepared in
91 a glycine buffer solution (Sigma-Aldrich, USA) in 30% absolute ethanol v/v (Sigma-Aldrich,
92 USA), whereas hydrochloric trace metal grade (Fisher Chemical, USA) and sodium
93 borohydride (Sigma-Aldrich, USA) were prepared in hydroxide solution (Fisher Chemical,
94 USA) for CV-AAS detection.

95

96 2.2 Synthesis of DTZc

97 Dicarboxylate 1,5-diphenyl-3-thiocarbazone (DTZc) was synthesized following the conditions
98 defined by Shenashen et al. [19]. Briefly, 1.9 g of hydrazinobenzoic acid were mixed with 0.6
99 mL of carbon disulfide, 20 mL of ethanol, 0.5 g of sodium hydroxide and 15 mL of distilled
100 water. The mixture was heated to reflux for 5 hours; then DTZc was precipitated as a white
101 solid by addition of ethanol, filtered, washed and dried. The reaction yield was 22% (0.95 g of
102 dicarboxylate 1,5-diphenyl-3-thiocarbazone).

103

104 2.3 Modification of 3D printed device

105 3D printed devices were post-processed by cleaning in isopropyl alcohol for 10 minutes and
106 curing for 1 hour under UV light. Integration of amine functions was carried out by immersion
107 of 3D printed post-cured parts for 1 h in a 10% m/v solution of hexane diamine prepared in a
108 solution of borate buffer adjusted to pH 11.5. The aminated parts were carefully cleaned by
109 successive baths in water, in ethanol and in water afresh. The DTZc grafting was then carried
110 out by immersion in a mixture of 5 g.L⁻¹ solution of N-(3-Dimethylaminopropyl)-N'-
111 ethylcarbodiimide (EDC), 5 g.L⁻¹ solution of 1-Hydroxybenzotriazole (HOBt) and 1 g.L⁻¹
112 solution DTZc in absolute ethanol for 30 min at room temperature. Modified supports were
113 then cleaned by successive immersions in water, in sodium hydroxide 10 mM, in water, in
114 ethanol and in water again, and kept at 4 °C until use.

115

116 2.4 Detection

117 Elution of modified supports after mercury extraction was carried out with a 0.5% m/v solution
118 prepared from L-cysteine.

119 For CV-AAS detection, a 6 mol.L⁻¹ solution of hydrochloric acid (trace metal grade) was used
120 with a 0.135 mol.L⁻¹ solution of sodium borohydride prepared in 0.125 mol.L⁻¹ sodium
121 hydroxide solution.

122 Concerning the colorimetric detection, a post-elution photo-oxidation step was first performed
123 using hydrogen peroxide and hydrochloric acid in order to obtain a final concentration of 0.5
124 mol.L⁻¹ of each reagent in the eluent. At the end of the photo-oxidation step, a 1.1 mol.L⁻¹
125 solution of ascorbic acid was then added to eliminate the excess of hydrogen peroxide before
126 detection. The final colorimetric reagent was prepared according to the conditions described by
127 Theraulaz et al. [20] with a 0.01 mmol.L⁻¹ solution of dithizone prepared in a 0.01 mol.L⁻¹
128 glycine buffer solution with 30% ethanol v/v, and mixed with a 0.001 mol.L⁻¹ thiourea solution
129 (Sigma-Aldrich, USA).

130

131 2.5. Apparatus

132 2.5.1. *Metal analysis*

133 Cold vapour atomic absorption spectrometry (CV-AAS) was used to quantify mercury in
134 standard solutions and real samples. The measurements were carried out on a Thermo Scientific
135 ICE3500 (USA) atomic absorption spectrometer equipped with a mercury hollow-cathode lamp
136 operated at 6 mA (wavelength of 253.7 nm) and a VP 100 Vapour System, with a peristaltic
137 pump operated at 30 rpm. Determinations were carried out with the following parameters: acid
138 flow rate 0.7 mL.min⁻¹, reductant flow rate 1.6 mL.min⁻¹, sample flow rate 7.0 mL.min⁻¹,
139 measuring time 6 seconds, argon flow rate 104 mL.min⁻¹.

140 Interferences of other metals on mercury extraction/elution were studied by inductively coupled
141 plasma–atomic emission spectrometry (ICP–AES) with a Jobin YVON JY2000 Ultratrace
142 spectrometer, equipped with a CMA spray chamber and a Meinhard R50-C1 glass nebuliser.
143 Determinations were performed with the following settings: power 1000W, pump speed 20
144 mL.min⁻¹, plasma flow rate 12 L.min⁻¹, coating gas flow rate 0.15 L.min⁻¹, nebuliser flow rate
145 1.08 L.min⁻¹ and nebuliser pressure 2.6 bar.

146

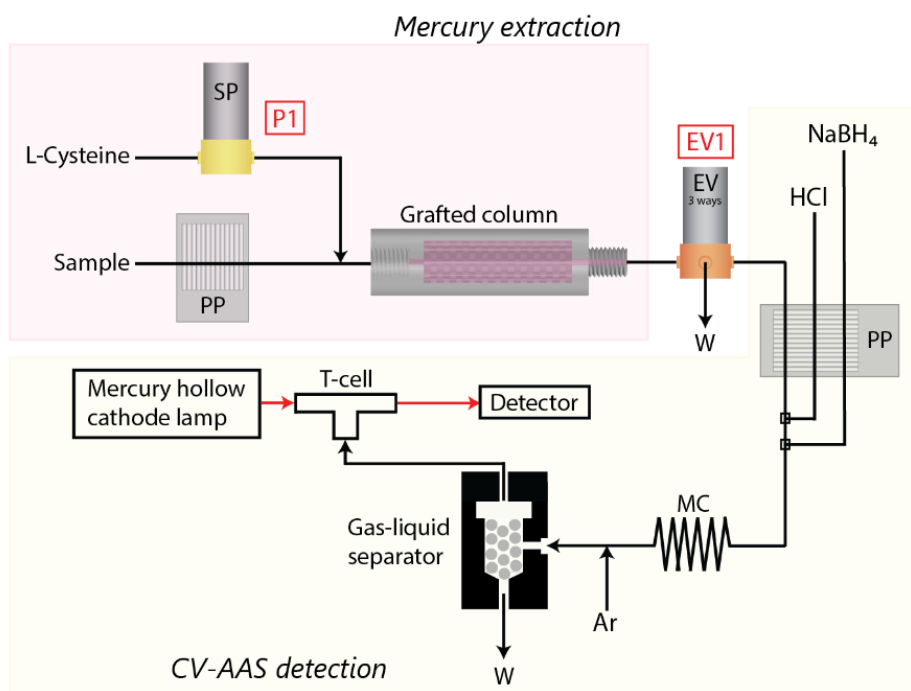
147 2.5.2. *3D printing*

148 The DTZc grafting procedure was optimized on 3D printed disks and cuboids. These pieces
149 were designed with Rhinoceros® 5.0 3D software (Robert McNeel & Associates Europe,
150 Spain) and then printed on the Form1+ stereolithographic printer (Formlabs, USA), using an
151 acrylate/methacrylate transparent resin (Clear, BV-002, Formlabs, USA). The integration of
152 amines functions and the DTZc grafting were first tested and optimized on 3D printed disks
153 (diameter 19 mm, thickness 2 mm) in batch experiments. Then the optimized parameters were
154 applied on a cuboids' column (14.1 x 54.1 mm, 284 cubes with a 1.5 mm diameter) which had
155 a grafted surface of 37.2 cm².

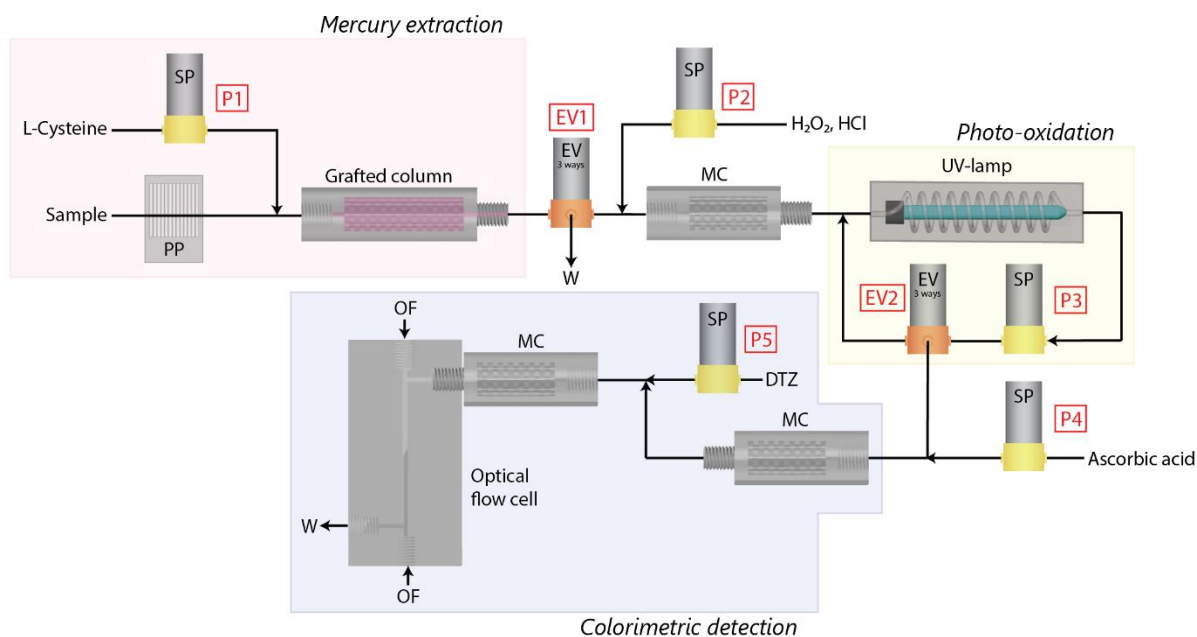
156

157 2.5.3. *Flow systems*

158 Sample was propelled using a peristaltic pump (Labcraft, Armtop, France). Reagents were
159 introduced by means of solenoid micro-pumps (Bio-ChemValve Inc., USA) with a stroke
160 volume of 20 µL and a highest frequency of 250 cycles/min and 3-way solenoid valves
161 (Takasago Electric Inc., Japan). The pumps and valves were computer-controlled by a
162 MCFIA/MPFS system (Sciware, Spain) with eight digital 12V output channels. Two flow
163 systems were developed according to the detection method used (CV-AAS or colorimetry),
164 their operating scheme is presented in Fig. 1 and Fig. 2.



165
 166 **Figure 1:** Flow system for mercury determination with CV-AAS detection [P1: solenoid micropump; PP:
 167 peristaltic pump; EV: solenoid valve; MC: mixing coil; W: waste; OF: optical fiber; Ar: argon].
 168



169
 170 **Figure 2:** Flow system for mercury determination with colorimetric detection [P1-P4: solenoid micropumps; PP:
 171 peristaltic pump; EV: solenoid valve; MC: mixing coil; W: waste; OF: optical fiber; DTZ: dithizone].
 172

173 In both systems, the first step of the analytical procedure was the mercury extraction from the
 174 sample (PP and EV1 to waste) on the DTZc grafted 3D printed cuboid column. Then, a solution
 175 of L-cysteine was pumped (P1) to elute the mercury extracted onto the grafted column.

176 The first system included a CV-AAS detection system directly after the elution step, previously
177 described in section 2.5.1 (Fig. 1).

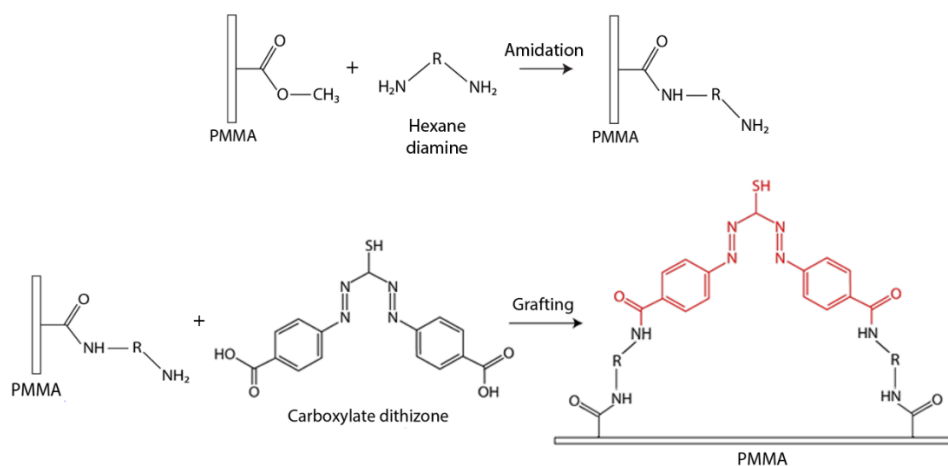
178 The second system offered a simple colorimetric detection (Fig. 2). This detection was based
179 on a photo-oxidation step to liberate the mercury from L-cysteine before a final colorimetric
180 detection with a dithizone reagent. A photo-oxidation module was used with a low-pressure
181 mercury lamp emitting at 254nm (90%) and 185 nm (10%), with a radiating part of 22.86 cm
182 in height and 0.95 cm in diameter, covered by a Suprasil quartz loop with an inner diameter of
183 2 mm (UVP PenRay, USA). Hydrogen peroxide oxidant solution (P2) was added to the eluate
184 to enhance photo-oxidation of L-cysteine and the mixture was exposed under UV-lamp for 30
185 minutes (P3 and EV2). An ascorbic acid solution (P4) was added at the end of this step to
186 eliminate excess of oxidant. The dithizone reagent (P5) was introduced in the system for the
187 detection of dithizone-mercury complex at 480 nm. Detection was carried out in a black 3D
188 printed spectroscopic flow-cell with a 5 cm optical pathlength. Two FC-UV600 optical fibers
189 (OF) (Ocean Optics, USA) were connected at the ends of optical pathlength, and isolated from
190 the reaction mixture with two tailor-made quartz discs, to guide the light from the source to the
191 spectrophotometric detector. The radiation of the halogen bulb of a DH-2000 UV-Vis light
192 source (Ocean Optics, USA) was transmitted to a USB2000 miniature spectrometer detector
193 (Ocean Optics, USA). The whole system was controlled by AutoAnalysis 5.0 software
194 (Sciware, Spain).

195

196 3. Results and discussion

197 3.1. Modification of 3D printed device

198 Stereolithography resins are mainly composed of methyl methacrylate, which is an ester
199 monomer. After photopolymerization and poly(methyl methacrylate) (PMMA) formation, this
200 ester group can be used to graft molecules onto the surface of 3D printed objects. This grafting
201 procedure requires two steps (global procedure is summarized in Fig. 3): first amine functions
202 were introduced onto 3D printed surface by amination reaction of the ester functions of the
203 PMMA with hexane diamine [21], followed by grafting of DTZc using an amidation reaction
204 with carboxylate function of DTZc. A pink coloration of the solid surface after cleaning at the
205 end of the procedure demonstrates efficiency of the DTZc grafting (supplementary materials
206 Fig. S1).



207

208 **Figure 3:** Grafting pattern of DTZc onto PMMA.

209 These two steps were optimized in batch experiments on 3D printed disks thanks to the results
 210 of ADECA test (Amino Density Estimation by Colorimetric Assay). This test allows
 211 quantification of the amine functions on a solid surface [22]. A chromogenic reagent, the
 212 Coomassie brilliant blue, reacts with amine functions in acidic medium. Then the quantity of
 213 Coomassie brilliant blue which has reacted with the amine functions is extracted in basic
 214 medium and finally quantified by colorimetric detection in acidic medium at a wavelength of
 215 611 nm.

216

217 3.1.1. PMMA amination step

218 The PMMA amination step was carried out according to the method previously described by
 219 Fixe et al. [21] with a heated solution of hexane diamine in borate buffer (pH=11.5). 3D printed
 220 disks were immersed in this solution with a reaction time between 30 min and 4 h. Three
 221 parameters were studied by a one-factor-at-a-time method: temperature, percentage of hexane
 222 diamine in solution, and time. The results of ADECA test obtained with the various operating
 223 conditions are summarized in Table 1 (the higher the result of ADECA test, the better the
 224 efficiency of the amination step). The results showed first the advantage of heating the hexane
 225 diamine solution to at least 50°C. There was no significant difference between 50 and 70°C
 226 with 1.42 ± 0.04 and 1.48 ± 0.05 respectively. Moreover, the 3D printed disks have shown signs
 227 of premature aging at 70°C with undesired cracking on the surface. Consequently, a temperature
 228 of 50°C was chosen as the optimal condition. Concerning the other parameters, a 10% m/v
 229 hexane diamine solution and a reaction time of 1 h were the best conditions to obtain a
 230 maximum amination efficiency (1.75 ± 0.13).

231

232

233 **Table 1.** Optimization of the PMMA amination reaction according to the ADECA test (n=3)

Operating conditions	Quantity of NH ₂ functions	
	ADECA test (a.u.)	
Temperature (°C)	25	1.26 ± 0.15
	50	1.42 ± 0.04
	70	1.48 ± 0.05
Hexane diamine concentration (% m/v)	10	1.75 ± 0.13
	15	1.43 ± 0.04
	20	1.41 ± 0.06
	25	1.24 ± 0.06
Amination time (h)	0.5	1.02 ± 0.06
	1	1.75 ± 0.13
	2	1.27 ± 0.02
	4	1.11 ± 0.05

234

235

236 3.1.2 DTZc grafting

237 The DTZc grafting was studied after amination of 3D printed disks according to the best
 238 operating conditions described previously. Four parameters have been optimized by a one-

239 factor-at-a-time method: activating agents (EDC and HOBt) concentration, DTZc
 240 concentration, temperature and grafting time. The influence of each parameter on the grafting
 241 efficiency was evaluated based on the results of the ADECA test. In this case, a low value of
 242 the ADECA test indicates a good efficiency of the grafting reaction, as it shows a decrease in
 243 the number of free amine groups onto the PMMA surface.

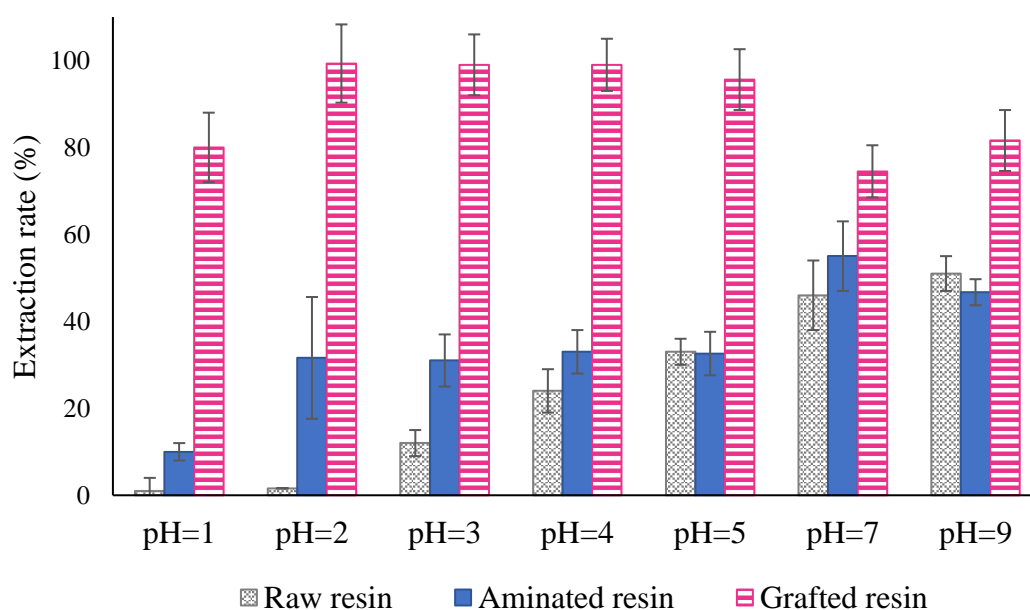
244 The results are summarized in Table 2. Concerning activating agents EDC and HOBt, a
 245 concentration of 5 g.L⁻¹ for both reagents was enough to obtain the best grafting rate (0.32 ±
 246 0.01). For the DTZc concentration, we observed no significant difference between 1 and 2.5
 247 g.L⁻¹ (with ADECA test results at 0.35 ± 0.02 and 0.33 ± 0.03 respectively). A concentration of
 248 1 g.L⁻¹ was thus selected for further experiments in order to limit the consumption of the reagent.
 249 No effect of temperature has been observed and the grafting reaction could therefore be
 250 performed at room temperature (25°C). Finally, a minimum reaction time of 30 min was
 251 necessary to obtain a good grafting efficiency and no significant difference was observed
 252 between 30 and 60 min.

253
 254 **Table 2.** Optimization of the PMMA grafting reaction [EDC: N-(3-Dimethylaminopropyl)-N'-ethylcarbodiimide;
 255 HOBt = 1-Hydroxybenzotriazole; DTZc = dicarboxylate 1,5-diphenyl-3-thiocarbazone] (n=3)

Operating conditions	Quantity of NH ₂ functions ADECA test (a.u.)	
EDC/HOBt concentration (g.L ⁻¹)	5	0.32 ± 0.01
	10	0.37 ± 0.03
	20	0.37 ± 0.05
	40	0.38 ± 0.03
DTZc concentration (g.L ⁻¹)	1	0.35 ± 0.02
	2.5	0.33 ± 0.03
	5	0.43 ± 0.02
	10	0.77 ± 0.04
Temperature (°C)	25	0.35 ± 0.02
	40	0.35 ± 0.02
	60	0.37 ± 0.02
Grafting time (min)	10	0.80 ± 0.11
	30	0.31 ± 0.02
	60	0.31 ± 0.02

256
 257
 258 **3.2. Solid phase extraction of mercury on grafted 3D printed device**
 259 *3.2.1 Extraction of metals*
 260 Shenashen et al. [19] have previously demonstrated that mercury was bonded to two molecules
 261 of DTZc through S and one N atom, which is consistent with dithizone reactivity, a well-known
 262 ligand which forms ML₂ complexes with various metals (including mercury) through S and N
 263 bonding.

264 After the optimization of the grafting procedure, mercury extraction was studied following
 265 various conditions. Raw resin, aminated resin, and grafted resin disks were immersed for 1 h in
 266 a $100 \mu\text{g.L}^{-1}$ mercury solution in PTFE tubes, at pH values between 1 and 9. The mercury
 267 solution was analysed by CV-AAS before and after extraction. The results obtained (extraction
 268 rate calculated from the concentrations before and after extraction) are summarized in Fig. 4.
 269 For pH value above 4, an average extraction of 38% of mercury by raw resin was observed (min
 270 24% at pH = 4; max 51% at pH = 9), which is characteristic of the adsorption of a metal on a
 271 plastic material surface, as it was previously demonstrated for polyethylene [23]. In acidic
 272 medium (pH=2), mercury was thus not extracted by the raw resin material (less than 1%): this
 273 result shows the importance to work at acidic pH to avoid the contamination of 3D printed
 274 pieces during the flow procedure. Aminated resin disks also showed a partial extraction of
 275 mercury in a pH range between 2 and 9, probably due to the complexation of mercury by the
 276 amine functions (min 32% at pH = 2, max 55% at pH = 7).
 277

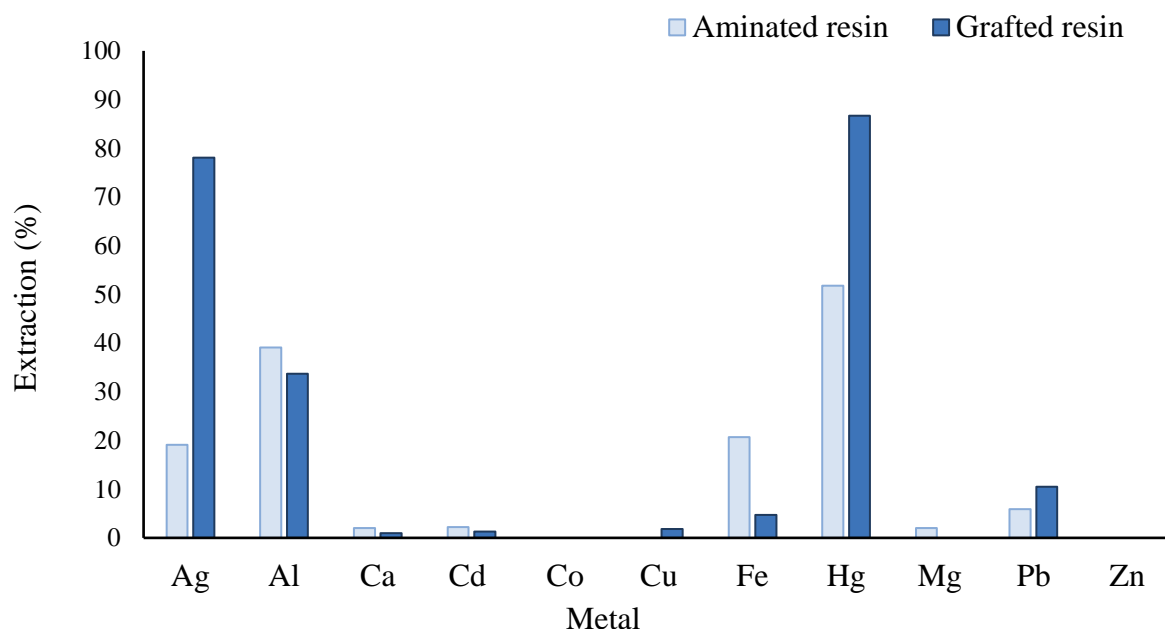


278
 279 **Figure 4:** Batch extraction of a $100 \mu\text{g.L}^{-1}$ mercury solution ($V=50 \text{ mL}$) on raw resin, aminated resin and DTZc
 280 grafted resin disks versus pH ($n=3$).
 281

282 Results showed complexation of mercury by DTZc onto the surface of disks, as shown by the
 283 significant increase of extraction rate between the raw resin disks and the grafted resin disks at
 284 acidic pH values. Concerning the grafted resin disks, the extraction in acidic medium was very
 285 efficient, with a mercury extraction rate of 99%. The acidification of the samples at pH=2 before
 286 extraction by the grafted resin was the best compromise to obtain good extraction performance
 287 and to avoid adsorption phenomena on the plastic surfaces. At this pH value, extraction kinetics
 288 was rapid since a mercury extraction rate of 90% was reached after a contact time of 1 minute
 289 (supplementary materials Fig. S2).

290 The selectivity of the DTZc grafted resin was tested with a multi-metal solution (aluminium,
 291 calcium, cadmium, cobalt, copper, iron, lead, magnesium, mercury, silver and zinc) at pH=2.
 292 This solution was extracted on the aminated and the grafted resins, and solutions were analysed

293 by ICP-AES before and after extraction (Fig. 5). The results showed a good extraction of silver,
 294 a partial extraction of aluminium and a low extraction of lead both for aminated and grafted
 295 resins. Iron was also partially extracted on the aminated resin (20%), but extraction rate on
 296 DTZc grafted resin was below 5%.
 297



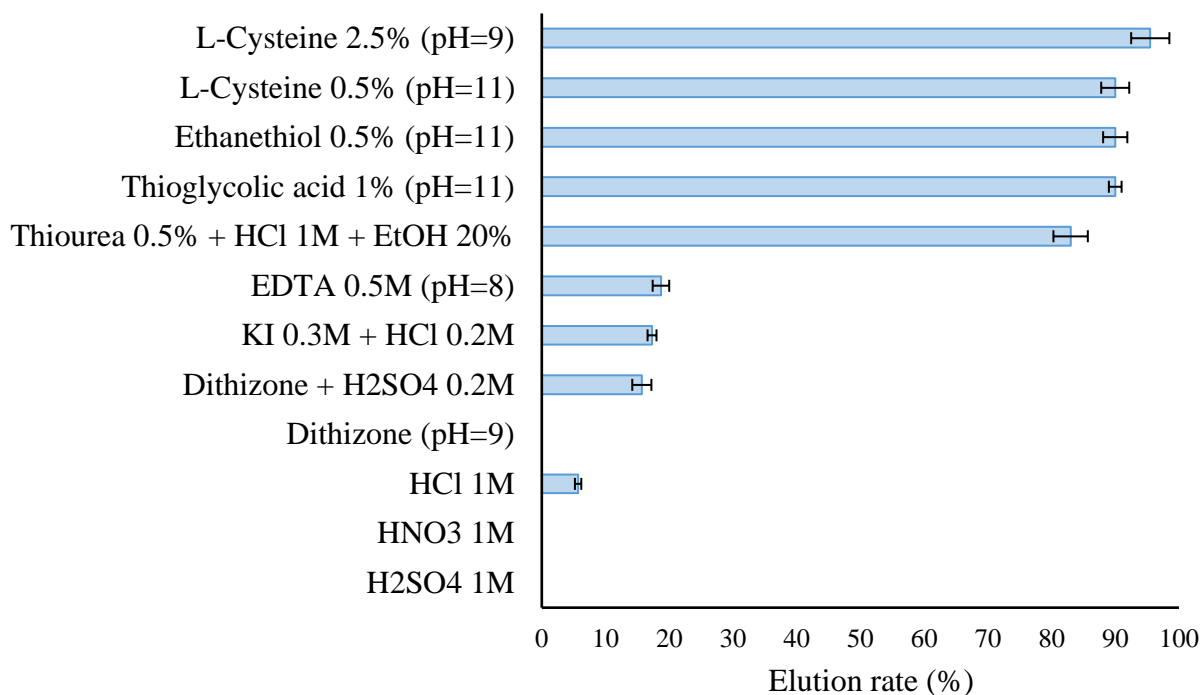
298
 299 **Figure 5:** Batch extraction of a multi-metal solution at $10 \mu\text{mol.L}^{-1}$ (aluminium, calcium, cadmium, cobalt, copper,
 300 iron, lead, magnesium, mercury, silver, and zinc; $V=50 \text{ mL}$) at $\text{pH}=2$ on the aminated resin disks and the grafted
 301 resin disks.
 302

303 Three metals presented thus a noticeable affinity with the DTZc grafted resin: silver, aluminium
 304 and lead. These interferences will be eliminated during the detection step: in the first flow
 305 system the colorimetric dithizone reagent contains a masking agent (thiourea) to limit foreign
 306 ions interferences, especially for silver, and in the second system the CV-AAS is a selective
 307 analytical method for Hg.
 308

309 3.2.2 Elution

310 After the extraction step, it was necessary to find a suitable eluent to recover the mercury
 311 extracted by the DTZc grafted resin. Several reagents were studied, and the tests are
 312 summarized in Fig. 6 (elution rates were calculated by the difference between the amount of
 313 mercury extracted on the grafted supports and the amount of mercury in the eluate solutions).
 314 Inorganic acids (hydrochloric, sulfuric and nitric acid), which are well known eluents for
 315 metals, were not efficient to elute mercury, even with 1 mol.L^{-1} concentration (higher
 316 concentrations were not tested to avoid the 3D resin degradation). Dithizone, EDTA and
 317 potassium iodide were also tested, but resulted respectively in 16%, 19% and 18% elution rates.
 318 Several eluents with thiol or thiocarbonyl functions were also studied: L-cysteine, ethanethiol,
 319 thioglycolic acid and thiourea. These four reagents were very efficient to elute mercury with
 320 elution rates higher than 90 %, except thiourea with 83%. These results are consistent with the
 321 high mercury affinity for thiolate compounds (R-SH) [24]. Recently Liem-Nguyen et al. [25]
 322 determined a formation constant of Hg(L)_2 complexes with cysteine and thioglycolic acid of

323 41.5 and 37.5 respectively. The three thiol compounds tested showed almost identical elution
 324 rates, and L-cysteine was chosen for further experiments as the least toxic and malodorous
 325 sulfur compound.
 326



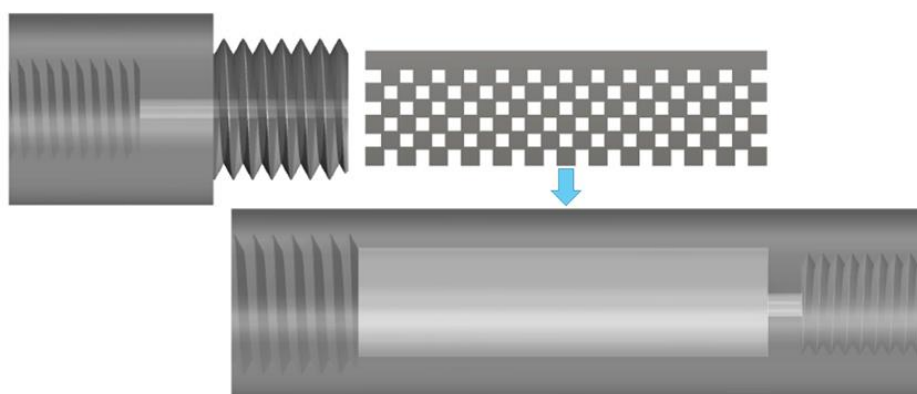
327
 328 **Figure 6:** Batch elution of mercury extracted on DTZc grafted resin with different eluents (V=50 mL; n=3).
 329

330 3.3. Application

331 3.3.1. Off-line sampling

332 Given the difficulties of on-site analysis of mercury and real sample storage for further
 333 laboratory analysis, a cuboid column was used to carry out on-site mercury extraction. For this
 334 purpose, a column was developed to incorporate a removable rectangular assembly of grafted
 335 cuboids (Fig. 7), these latter ones being able to be changed for each sample.
 336

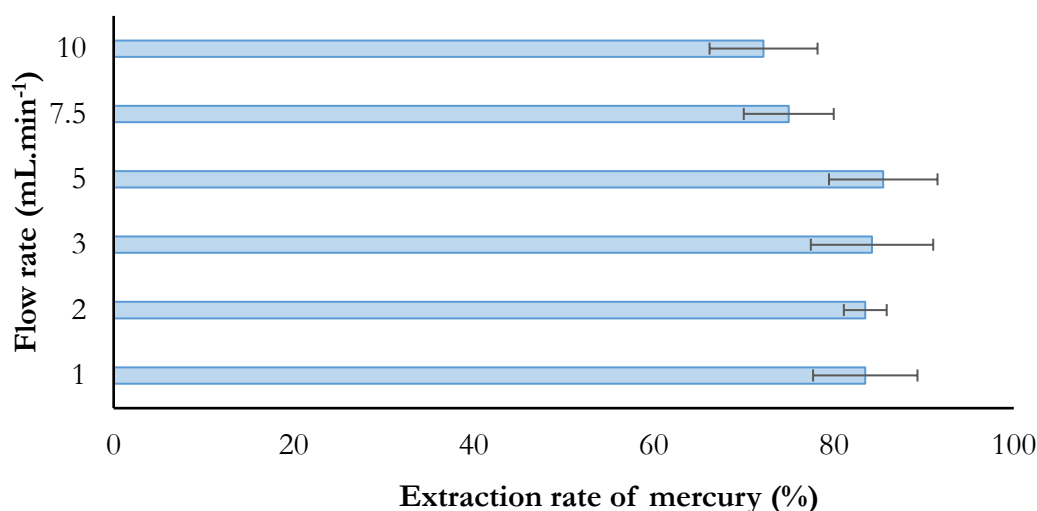
337



338
 339 **Figure 7:** Scheme of removable column of grafted cuboids.
 340

341
 342

343 To optimize the efficiency of the extraction step, the mercury extraction flow rate was studied
 344 between 1 and 10 mL.min⁻¹ by means of a peristaltic pump. The results are depicted in Fig. 8.
 345 Flow rate showed no significant effect on extraction rate between 1 and 5 mL.min⁻¹ with an
 346 average mercury extraction rate of 85%. Comparison of extraction efficiency versus higher
 347 sample flow rates showed a 12% and 17% decrease respectively for sample flow rates of 7.5
 348 mL.min⁻¹ (mercury extraction rate of 75%) and 10 mL.min⁻¹ (mercury extraction rate of 72%).
 349 Nevertheless, despite the 17% loss, a sample flow rate of 10 mL.min⁻¹ could be a good
 350 compromise between the extraction efficiency and the extraction time (or sample volume). A
 351 sample flow rate of 10 mL.min⁻¹ enables in a given time a significant increase of the
 352 preconcentration factor by percolating higher volumes of sample. For a 1 h sample percolation,
 353 a preconcentration factor of 23 is thus obtained for a sample flow rate of 5 mL.min⁻¹ versus 38
 354 for a sample flow rate of 10 mL.min⁻¹.
 355



356
 357 **Figure 8:** Influence of flow rate on the extraction of a 100 µg.L⁻¹ mercury solution in a grafted cuboids column
 358 (n=3).
 359

360 After the extraction step, the entire cuboids assembly can be removed from the column and
 361 introduced in a nickel boat of a mercury analyzer Altec AMA 254 which is specifically
 362 conceived for the fast, precise and simple determination of mercury traces in solids samples.
 363 Note that with this technique, it was necessary to perform a blank on grafted cuboids before
 364 extraction, because the analysis of the raw resin used for 3D printing has showed a mercury
 365 concentration of 9.6 ± 3.2 ng.g⁻¹.
 366

367 3.3.2. Flow systems

368 Mercury can also be quantified in solution after elution by L-cysteine by CV-AAS (Fig. 1). As
 369 the mercury concentration is usually low in environmental samples, it is necessary to work with
 370 large sample volumes to achieve a large preconcentration factor. In this study, the sample
 371 volume was set at 500 mL to limit the analysis time (mercury extraction was successfully tested
 372 for sample volumes up to 1 L). Experiments were carried out to determine the minimum volume
 373 of L-cysteine which has to be used to quantitatively elute the mercury extracted on modified
 374 supports. Results showed that a minimum volume of 10 mL of 0.5% m/v L-cysteine in borate

375 buffer (pH=11) should be used to elute 92% of the mercury extracted on the modified support
376 (Supplementary materials, Figure S3).

377 The analytical features of this procedure were thus determined for a sample volume of 500 mL
378 and an elution volume of 10 mL: a limit of detection (LOD, 3σ ; $n=10$) of 2.6 ng.L^{-1} and a limit
379 of quantification (LOQ, 10σ ; $n=10$) of 8.6 ng.L^{-1} were achieved, with a linear range from 8.6
380 to 200 ng.L^{-1} . The overall analysis time by this analytical procedure was 60 minutes. The 3D
381 printed DTZc grafted supports can be reused for 3 successive extractions. The tests showed a
382 decrease in the extraction rate to 65% from the fourth extraction. This method was validated on
383 two samples of fresh water and drinking water: as the mercury concentration was below the
384 LOD, samples were spiked to 40 ng.L^{-1} . The results obtained were consistent with 38.2 ± 5.1
385 ng.L^{-1} for fresh water and $44.1 \pm 4.2 \text{ ng.L}^{-1}$ for drinking water (recovery rates ranged from 83%
386 to 120% in sample replicates).

387 The analytical procedure of the second flow system (Fig. 2) was divided in four steps: extraction
388 of mercury, elution, photo-oxidation, and colorimetric detection. Dithizone reagent was used
389 for the mercury detection because of its sensibility to mercury and to avoid interferences with
390 other extracted metals (silver and aluminium). A linear domain was observed between 1 and
391 $200 \text{ }\mu\text{g.L}^{-1}$ for a 500 mL sample volume and a 10 mL elution volume. The limit of detection
392 was $0.3 \text{ }\mu\text{g.L}^{-1}$ ($n=10$), and the limit of quantification was $1.0 \text{ }\mu\text{g.L}^{-1}$. Coefficient of variation
393 obtained for a mercury concentration of $50 \text{ }\mu\text{g.L}^{-1}$ was 2.2%. The overall analysis time by this
394 analytical procedure was 90 minutes.

395 Given these results, the flow system with colorimetric detection was more intended for analysis
396 of wastewater or industrial water, while the CV-AAS flow system was most adapted for fresh
397 water and seawater because of its lower LOD and LOQ.

398

399 **Conclusion**

400 In this study, a new possibility offered by 3D printing has been explored. The
401 acrylate/methacrylate resin can be used as an inert support to graft selective molecules. The two
402 steps of the grafting procedure were developed and optimized. The first step was the integration
403 of amine functions on PMMA, followed by reaction between these amine functions and the
404 carboxylate function of DTZc. A very good extraction of mercury was observed, and the grafted
405 resin can be eluted with thiol eluents, more particularly with L-cysteine, which has a high
406 affinity with mercury.

407 A 3D printed column of cuboids has been grafted and several applications of this module have
408 been presented to show the different opportunities of the grafting of 3D resin. Other molecules
409 with carboxylate functions could also be grafted by the same procedure for the extraction of
410 various metals. This type of column (cubes were spaced 1.2 mm from each other) could lead to
411 many advantages for solid phase extraction: no clogging, use of unfiltered or prefiltered samples
412 and compatibility with high flow rates.

413

414 **Acknowledgment**

415 This work was included in the project “Lab-on-Ship” funded by the French Research Agency
416 (ANR-14-CE04-0004). The authors are thankful to Françoise Marco-Miralles and Michelle
417 Brochen from IFREMER for Hg analysis with Altec AMA 254.

418

419 **References**

- 420 [1] E. Pelletier, Mercury-selenium interactions in aquatic organisms: A review, *Marine*
421 *Environmental Research*. 18 (1986) 111–132. doi:10.1016/0141-1136(86)90003-6.
- 422 [2] Cancer du poumon et exposition professionnelle aux métaux : une revue des études
423 épidémiologiques - Article de revue - INRS, (2018).
424 <http://www.inrs.fr/media.html?refINRS=TC%20120> (accessed April 16, 2018).
- 425 [3] C. Freire, R. Ramos, M.-J. Lopez-Espinosa, S. Díez, J. Vioque, F. Ballester, M.-F.
426 Fernández, Hair mercury levels, fish consumption, and cognitive development in preschool
427 children from Granada, Spain , *Environmental Research*. 110 (2010) 96–104.
428 doi:10.1016/j.envres.2009.10.005.
- 429 [4] T. Yorifuji, T. Tsuda, S. Inoue, S. Takao, M. Harada, Long-term exposure to
430 methylmercury and psychiatric symptoms in residents of Minamata, Japan, *Environment*
431 *International*. 37 (2011) 907–913. doi:10.1016/j.envint.2011.03.008.
- 432 [5] Prévention du risque chimique - Mercure, cycle et toxicité, (2018).
433 <http://www.prc.cnrs.fr/spip.php?rubrique42> (accessed April 25, 2018).
- 434 [6] J.C. Varekamp, P.R. Buseck, Global mercury flux from volcanic and geothermal
435 sources, *Applied Geochemistry*. 1 (1986) 65–73. doi:10.1016/0883-2927(86)90038-7.
- 436 [7] S. Tang, X. Feng, J. Qiu, G. Yin, Z. Yang, Mercury speciation and emissions from coal
437 combustion in Guiyang, Southwest China., *Environ Res*. 105 (2007) 175–182.
438 doi:10.1016/j.envres.2007.03.008.
- 439 [8] D.G. Streets, Z. Lu, L. Levin, A.F.H. ter Schure, E.M. Sunderland, Historical releases
440 of mercury to air, land, and water from coal combustion, *Science of The Total Environment*.
441 615 (2018) 131–140. doi:10.1016/j.scitotenv.2017.09.207.
- 442 [9] D.G. Streets, H.M. Horowitz, D.J. Jacob, Z. Lu, L. Levin, A.F.H. Ter Schure, E.M.
443 Sunderland, Total Mercury Released to the Environment by Human Activities, *Environ. Sci.*
444 *Technol*. 51 (2017) 5969–5977. doi:10.1021/acs.est.7b00451.
- 445 [10] A.N. Anthemidis, G.A. Zachariadis, J.A. Stratis, Development of a sequential injection
446 system for trace mercury determination by cold vapour atomic absorption spectrometry
447 utilizing an integrated gas–liquid separator/reactor, *Talanta*. 64 (2004) 1053–1057.
448 doi:10.1016/j.talanta.2004.05.003.
- 449 [11] H. Erxleben, J. Ruzicka, Atomic Absorption Spectroscopy for Mercury, Automated by
450 Sequential Injection and Miniaturized in Lab-on-Valve System, *Analytical Chemistry*. 77
451 (2005) 5124–5128. doi:10.1021/ac058007s.
- 452 [12] L.O. Leal, O. Elsholz, R. Forteza, V. Cerdà, Determination of mercury by multisyringe
453 flow injection system with cold-vapor atomic absorption spectrometry, *Analytica Chimica*
454 *Acta*. 573–574 (2006) 399–405. doi:10.1016/j.aca.2006.04.078.
- 455 [13] M. Garrido, M.S. Di Nezio, A.G. Lista, M. Palomeque, B.S. Fernández Band, Cloud-
456 point extraction/preconcentration on-line flow injection method for mercury determination,
457 *Analytica Chimica Acta*. 502 (2004) 173–177. doi:10.1016/j.aca.2003.09.070.
- 458 [14] J.F. van Staden, R.E. Taljaard, Determination of Lead(II), Copper(II), Zinc(II),
459 Cobalt(II), Cadmium(II), Iron(III), Mercury(II) using sequential injection extractions, *Talanta*.
460 64 (2004) 1203–1212. doi:10.1016/j.talanta.2004.06.020.

- 461 [15] C. R. Hammerschmidt, K. L. Bowman, M.D. Tabatchnick, C. H. Lamborg, Storage
462 bottle material and cleaning for determination of total mercury in seawater, *Limnol. Oceanogr.:*
463 *Methods* 9 (2011) 426-431. doi:10.4319/lom.2011.9.426
- 464 [16] E. Mattio, F. Robert-Peillard, C. Branger, K. Puzio, A. Margaillan, C. Brach-Papa, J.
465 Knoery, J.-L. Boudenne, B. Coulomb, 3D-printed flow system for determination of lead in
466 natural waters, *Talanta*. 168 (2017) 298–302. doi:10.1016/j.talanta.2017.03.059.
- 467 [17] E. Mattio, F. Robert-Peillard, L. Vassalo, C. Branger, A. Margaillan, C. Brach-Papa, J.
468 Knoery, J.-L. Boudenne, B. Coulomb, 3D-printed lab-on-valve for fluorescent determination
469 of cadmium and lead in water, *Talanta*. 183 (2018) 201–208. doi:10.1016/j.talanta.2018.02.051.
- 470 [18] C. Calderilla, F. Maya, V. Cerdà, L.O. Leal, 3D printed device for the automated
471 preconcentration and determination of chromium (VI), *Talanta*. 184 (2018) 15–22.
472 doi:10.1016/j.talanta.2018.02.065.
- 473 [19] M.A. Shenashen, S.A. El-Safy, E.A. Elshehy, Architecture of optical sensor for
474 recognition of multiple toxic metal ions from water, *Journal of Hazardous Materials*. 260 (2013)
475 833–843. doi:10.1016/j.jhazmat.2013.06.025.
- 476 [20] F. Théraulaz, O.P. Thomas, Complexometric determination of mercury(II) in waters by
477 spectrophotometry of its dithizone complex, *Microchimica Acta*. 113 (1994) 53–59.
478 doi:10.1007/BF01243137.
- 479 [21] F. Fixe, M. Dufva, P. Telleman, C.B.V. Christensen, Functionalization of poly(methyl
480 methacrylate) (PMMA) as a substrate for DNA microarrays, *Nucleic Acids Res.* 32 (2004) e9.
481 doi:10.1093/nar/gng157.
- 482 [22] G. Coussot, C. Perrin, T. Moreau, M. Dobrijevic, A. Le Postollec, O. Vandenabeele-
483 Trambouze, A rapid and reversible colorimetric assay for the characterization of aminated solid
484 surfaces, *Anal Bioanal Chem.* 399 (2011) 1061–1069. doi:10.1007/s00216-010-4363-7.
- 485 [23] A. Turner, L.A. Holmes, Adsorption of trace metals by microplastic pellets in fresh
486 water, *Environ. Chem.* 12 (2015) 600–610. doi:10.1071/EN14143.
- 487 [24] P. Pohl, B. Prusisz, Preconcentration of Mercury Using Duolite GT-73 in the Analysis
488 of Water Samples by Inductively Coupled Plasma Atomic Emission Spectrometry, *Analytical*
489 *Sciences*. 20 (2004) 1367–1370. doi:10.2116/analsci.20.1367.
- 490 [25] V. Liem-Nguyen, U. Skyllberg, K. Nam, E. Björn., Thermodynamic stability of
491 mercury(II) complexes formed with environmentally relevant low-molecular-mass thiols
492 studied by competing ligand exchange and density functional theory, *Environmental Chemistry*
493 14 (2017) 243-253doi:10.1071/EN17062.
- 494

Modified 3D-printed device for mercury determination in waters

Supplementary Materials

Elodie Mattio¹, Nadia Ollivier¹, Fabien Robert-Peillard¹, Robert Di Rocco¹, Catherine Branger², André Margaillan², Christophe Brach-Papa³, Joël Knoery³, Damien Bonne⁴, Jean-Luc Boudenne¹, Bruno Coulomb^{1*}

¹ Aix Marseille Univ, CNRS, LCE, Marseille, France.

² University of Toulon, MAPIEM, La Garde, France.

³ IFREMER, LBCM, Nantes, France.

⁴ Aix Marseille Univ, CNRS, Centrale Marseille, ISM2, Marseille, France.

*Corresponding author: bruno.coulomb@univ-amu.fr

Full postal address: LCE, Case 29, 3 place Victor Hugo, 13331 Marseille cedex 3, France.

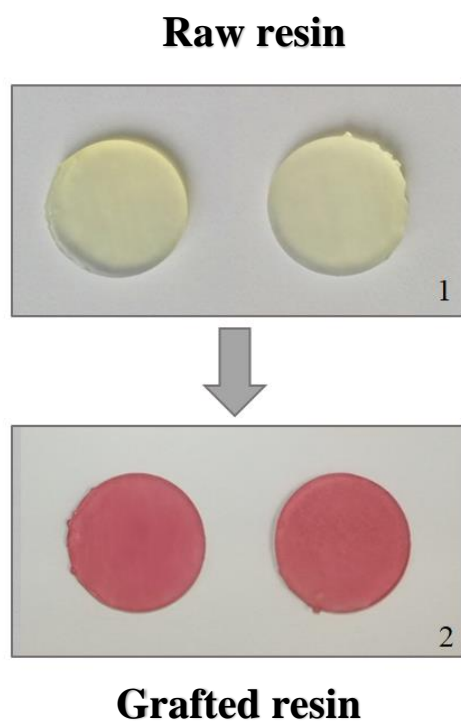
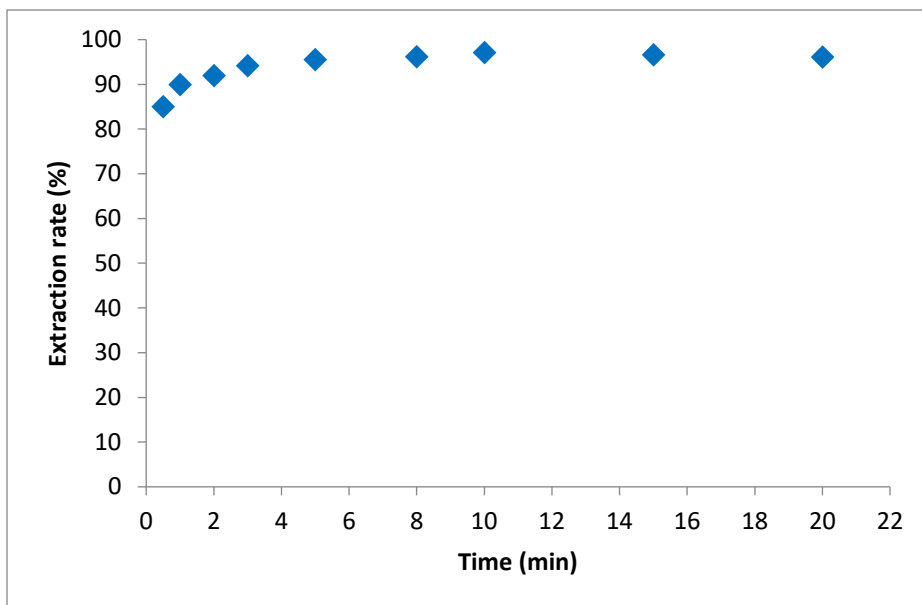
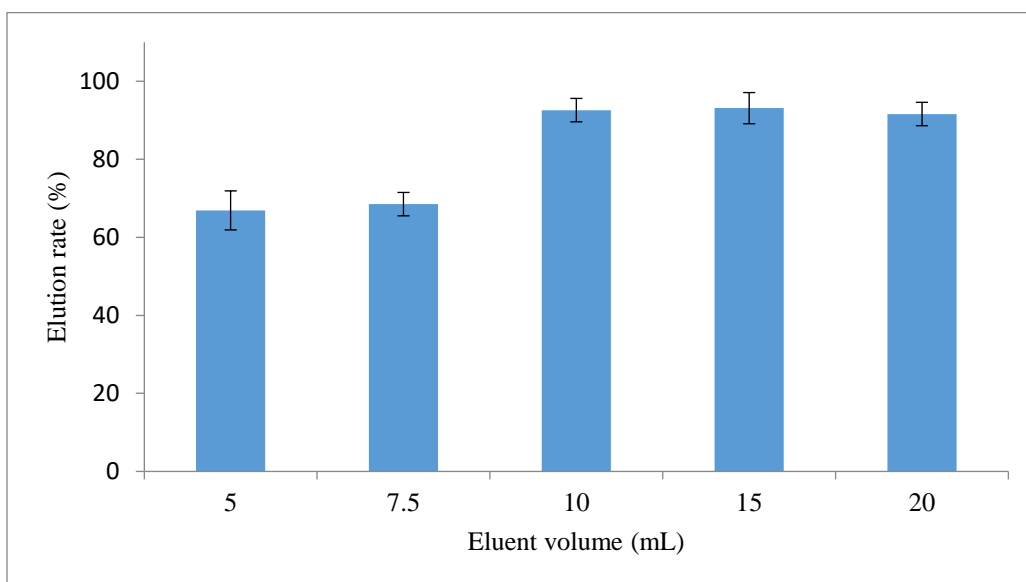


Figure S1: Pictures of 3D printed objects during grafting steps (1: raw resin disks; 2: grafted resin disks; 3: grafted cuboids columns).



525
526 Figure S2: Extraction rate versus contact time at pH=2.

527
528



529
530 Figure S3: Elution rate by L-cysteine versus eluent volume (L-cysteine 0.5% m/v in 100 mM
531 borate buffer pH=11).

532
533
534
535
536
537